International Conference on Applied Energy 2020
Dec. 1 - Dec. 10, 2020, Bangkok / Virtual
Paper ID: 677

Optimization under uncertainty of biogas-fueled solid oxide fuel cell system

Yash Khanna[1], David Tucker[2], Valentina Zaccaria [1*]

1 Mälardalen University, School of Business, Society and Engineering

2 U.S. Department of Energy, National Energy Technology Laboratory

*Corresponding Author: valentina.zaccaria@mdh.se

ABSTRACT

Solid oxide fuel cell systems operating with biogas can be considered an efficient solution for carbon-free energy conversion. Given the efficiency levels at small-scale, a 100 kW range cogenerative system for micro-grid applications was considered in this study. The challenge in employing biomass-derived fuel in solid oxide fuel cells is related to the performance fluctuations due to biomass intrinsic variability. Thus, the exact composition of the fuel may vary in unpredicted ways during the fuel cell lifetime. An uncertainty analysis combined with a design optimization study was conducted on the fuel cell system and it was demonstrated that the deviation in rate of return is statistically significant, and thus robust optimization is needed for designing a system fueled with highly variable biogas composition.

Keywords: solid oxide fuel cell, biogas, genetic algorithm, uncertainty analysis

NONMENCLATURE

Abbreviations	
FU	Fuel utilization
GA	Genetic algorithm
IRR	Internal rate of return
MBC	Model based calibration
NAP	Net annual profit
SOFC	Solid oxide fuel cell
TCI	Total capital investment
Symbols	
I	Current [A]
m	Mass flow rate [kg/s]
P	Power [kW]
T	Temperature [K]
V	Voltage [V]

1. INTRODUCTION

Solid oxide fuel cells (SOFCs), with their high operating temperature and capability to operate with various fuels, are a key technology for enabling the shift toward a zero-carbon society. The electrical efficiency when operating with hydrogen has been proven higher than 60% even in small-scale applications [1]. Even in absence of a hydrogen infrastructure, SOFCs can function with natural gas or other hydrocarbon fuels due to the desirable conditions for internal methane reforming and water gas shifting [2]. SOFCs have attracted considerable attention for cogeneration applications in micro-grid and residential sector [3-5].

The use of biogas is of particular interest to reduce carbon emissions. Biogas can be produced through a process of gasification of biomass, such as wood, organic waste, etc. Gasification occurs at high temperature (>700°C) and limited oxygen availability, which results in a synthetic gas that is a mixture of CH_4, H_2, CO, CO_2, and H_2O with traces of nitrogen and other compounds. The exact composition depends significantly on the gasification technology, the type of biomass, and the operating conditions. Due to the intrinsic variability in biomass characteristics (e.g. moisture content, nitrogen content etc.), we can expect a variation in biogas composition even when all the other conditions are the same [6, 7]. Fluctuations in fuel compositions were shown to affect the performance of a fuel cell system fed with biogas [8].

Due to high operation temperature range the exhaust gas from the SOFC stack is often self-sufficient for spontaneous burning in a post-combustor. Use of cogeneration technologies like SOFC-CHP and SOFC-GT can enhance the system efficiency by utilizing this exhaust heat. A genetic algorithm based multi-objective optimization estimated an achievable efficiency of 63% for a biogas fueled SOFC-GT system [9]. A thermodynamic and economic optimization of SOFC coupled with gas turbine and steam turbine showed a system efficiency higher than 70% when fed with syngas from heavy oil gasification [10]. Multi-objective optimization was used to demonstrate an efficiency above 70% when combining SOFC, GT, and gasification of lignocellulosic biomass [11]. None of these studies however considered possible fluctuations in biogas quality during system operations.

The goal of this work is to optimize the design of a SOFC system operating with biogas for micro-grid applications, under the consideration of fluctuating biogas composition.

$$\eta = (P_e * \eta_{inverter} * \eta_{generator} + \dot{Q}_{net})/(\dot{m}_f * LHV).$$

The system in exam was a 100-500 kWe range SOFC for micro-grid applications fed with biogas, whose composition is shown in Table 1. Expected range of variation in the biogas composition is also presented [14-16].

Table 1. Biogas composition from a dual bed gasifier

	Mole fraction [%]	Expected variation [%]
CH_4	9.1	0-15
H_2	15	10-30
CO	24.7	20-50
CO_2	7.1	5-15
H_2O	42	30-50
N_2	2.1	0-5

2.1 Data preparation

Response	Predictors	Function	R^2	
T_{cell}	$I\ ,T_{ai}\ ,\dot{m}_a$	$T_{cell} = f(I^3,\ {T_{ai}}^3, {\dot{m}_a}^3)$	0.996	
V_{cell}	I, T_{cell}	$V_{cell} = f(I, {T_{cell}}^3)$	0.97	
FU	$I, \dot{m}_{fuel_{percell}}$	$FU = f(I, \dot{m}_{f_{percell}})$	0.991	
$\dot{H}_{FC}$	$T_{ai}\ ,\dot{m}_a$	$\dot{H}_{FC} = f(\ {T_{ai}}^2, {\dot{m}_a}^2)$	1	
$\dot{H}_{PC}$	$FU, T_{ai}\ ,\dot{m}_a$	$\dot{H}_{PC} =\ f(FU^3,\ {T_{ai}}^3, {\dot{m}_a}^3)$	0.975	

Table 2. Response function characteristics

2. METHODOLOGY

The SOFC system was modeled in MATLAB-Simulink as a 1D model of a stack of planar, co-flow SOFCs, and a lumped model of post-combustor and heat exchangers as in [12]. Since the complexity of the dynamic 1D model was too high for the optimization procedure, a surrogate model was built from data obtained through the dynamic model. The thermo-electric performance parameters of the surrogate SOFC model included the average cell temperature (T_{cell}), net cell voltage after considering overpotentials (V_{cell}), which can a function of cell temperature and current [13], fuel-utilization (FU), the enthalpy of air at inlet of fuel cell or pre heating enthalpy (H_{FC}), and the enthalpy generated at the outlet of post-combustor (H_{PC}). Further, the air preheating from ambient conditions to inlet of fuel cell was formulated with a physical equation of first law of thermodynamics, in the form:

$$\dot{Q}_{pre} = \ \dot{m}_a c_{pa}(T_{ai} - T_{amb}).$$

Here $\dot{m}_a$ is the cathode air mass flow rate, c_{pa} is the isobaric specific heat of air, T_{ai} is the inlet temperature of air to the FC and T_{am} is the ambient air. The system efficiency was calculated as:

The simulations on the dynamic model were performed under the assumptions of steady-state flow, constant fuel concentration, no cell degradation, and atmospheric pressure of air and fuel at the inlet. The input parameters or predictor variables were: the cathode T_{ai}, $\dot{m}_a$, the stack current I, and the anode fuel inlet mass flow rate $\dot{m}_f$. These predictors were varied using quasi-random sampling method to get the response variables of the training data set from the series of 1D SOFC model simulations. T_{cell}, V_{cell}, FU, H_{FC}, and H_{PC} were the essential response variables. The training data set comprised of a total 200 data points in the range of operations of the chosen system.

The Model Based Calibration (MBC) tool in MATLAB was used to develop the surrogate empirical functions. The predictor and response characteristics of the surrogate model functions is shown in Table 2. All functions developed were selected to be polynomials for simplicity, and the best fit was evaluated based on the value of R^2. 20% of data was taken for internal validation in the MBC tool while training the model functions.

Figures 1 and 2 show the predicted vs training values of the response parameters, which represents an indication of the accuracy of the surrogate functions compared to the dynamic 1D SOFC model.

A different set of validation dataset of predictor values was further used to estimate the relative error of the surrogate function values compared to the 1D SOFC model, the maximum value of which is shown in Table 3.

Table 3. Maximum relative error of the surrogate model

Variable	Maximum relative error
T_{cell}	4.09%
V_{cell}	4.88%
FU	3.83%
$\dot{H}_{FC}$	0.1%
$\dot{H}_{PC}$	10%

2.2 Optimization algorithm

The internal rate of return (IRR) of the system was selected as objective function for the optimization strategy. The IRR depends on the total capital investment (TCI) and the annual cashflows for all the years of the system lifetime:

$$\sum_{j=1}^{\text{Lifetime}} \frac{NAP_j}{(1+\text{IRR})^j} - \text{TCI} = 0$$

The cashflow is represented by the Net Annual Profit, given by:

$$NAP = C_{electricty} * E_{electrcity} + C_{heating} * E_{heating} - C_{Biogas} * E_{Biogas} - Cost_{O\&M}.$$

Here C is the cost of commodity in €/kWh and E is the commodity generated or consumed in kWh, $Cost_{O\&M}$ is the annual operation and maintenance cost. The total investment cost is represented as $TCI = C'_{inv} * P_e$ where C'_{inv} is the cost factor in €/kW$_{elec}$ and P_e is the electric power in kW. The set of constant assumptions in the optimization model are shown in Table 4.

Table 4. Assumed constants for the economic analysis

Biogas cost [17]	50 €/MWh
Electricity cost	0.15 €/kWh
Heat cost	0.1 €/kWh
Tamb	283 K
O&M cost	4% of C_{inv}
Inverter efficiency	92%
Generator efficiency	99%
Lifetime	20 years

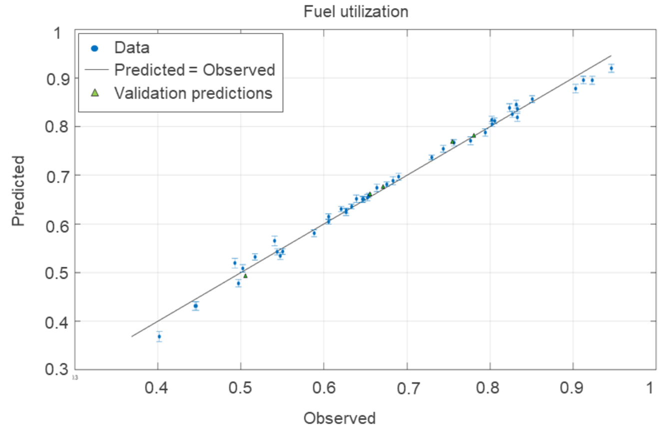

Fig. 1 – Fuel utilization model accuracy

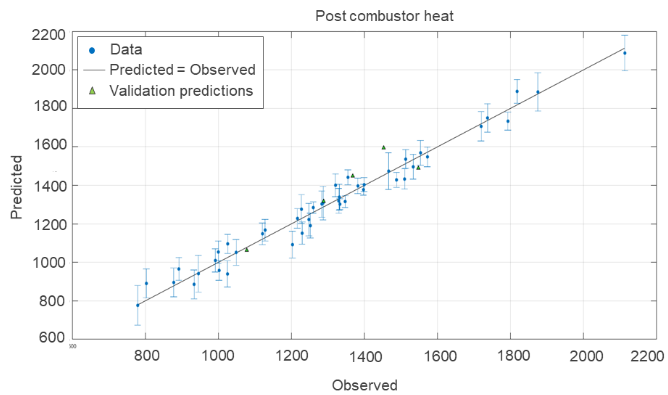

Fig. 2 – Post combustor heat model accuracy

For the total capital investment, two target values for SOFC system cost were assumed: a short-term target value of 2500 \$/kWe and a futuristic target of 900 \$/kWe [18].

The selected optimization algorithm was genetic algorithm (GA), with population per generation and maximum number of generations equal to 50 for both. The key inputs for the optimization are T_{ai}, $\dot{m}_a$, I, $\dot{m}_f$ and the number of cells N_{cells}. The ratio of $\dot{m}_f$ to N_{cells} is the input $\dot{m}_{f_{percell}}$ to the FU function. The GA changes these set of five inputs to achieve the best value for the objective functions over the iterations. The cells are connected in a series layout and the stack voltage can be given as $V_s = V_{cell} * N_{cells}$ and $P_e = V_s * I$. The optimization through the GA is summarized in Figure 3.

Lower and upper bounds were set in the optimization to limit the FU to 90%. The first reason was to remain in the range of validity of the model, and the second one to avoid risk of fuel starvation.

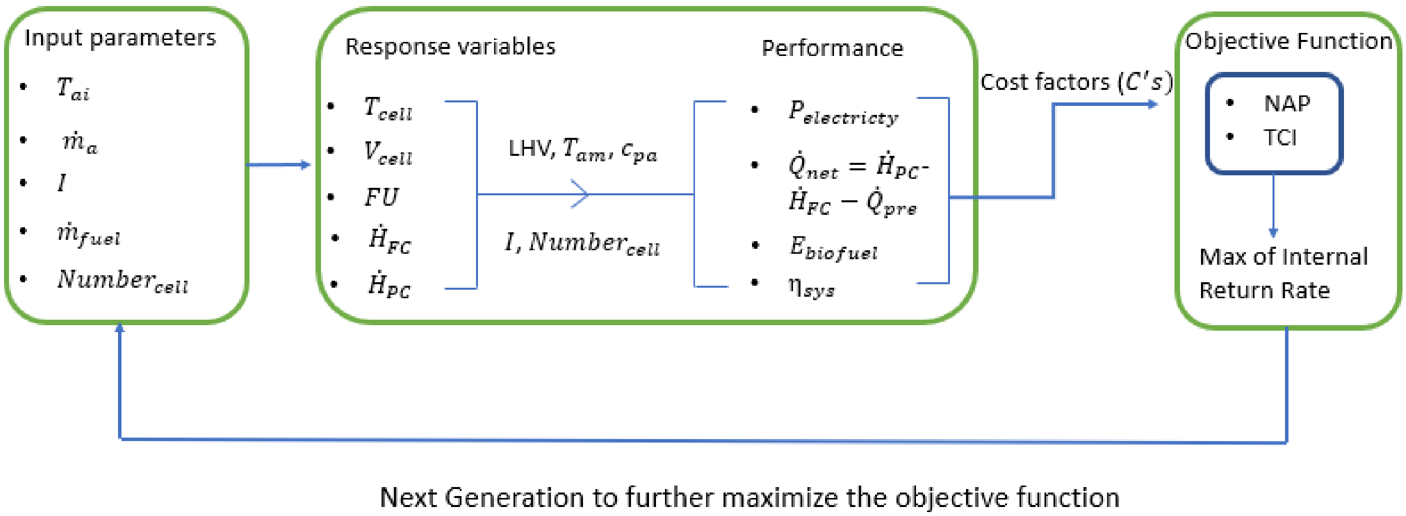

Figure 3. Schematic flow of the optimization process

3. RESULTS AND DISCUSSION

Six scenarios were simulated depending on the investment cost, electricity cost, and whether or not the SOFC system was operating in cogeneration mode. The scenarios named S1 to S6 and their specifications are illustrated in Table 5.

Table 5. Simulated scenarios

S1	Cogeneration, $C_{electricty} = 0.15$ $C'_{inv} = 900$
S2	Cogeneration, $C_{electricty} = 0.1$ $C'_{inv} = 2500$
S3	Cogeneration, $C_{electricty} = 0.15$ $C'_{inv} = 2500$
S4	Cogeneration, $C_{electricty} = 0.1$ $C'_{inv} = 900$
S5	$C_{electricty} = 0.15$ $C'_{inv} = 2500$
S6	$C_{electricty} = 0.15$ $C'_{inv} = 900$

Scenarios considering a low electricity price and no cogeneration showed to be unfeasible with a negative value of IRR, and therefore were not included. In fact, the minimum electricity price was calculated to be 0.12 €/kWh to guarantee the feasibility of the system with a low investment cost and 0.13 €/kWh if the TCI was 2500 \$/kWe.

The results of the optimization are presented in Table 6. The obtained optimal input parameters were used to run the dynamic 1D model and verify that the error on the output parameters was within the validation error. Further, the 1D model was used to verify that the temperature variation in the fuel cell stack was always below 6.3 K/cm for all the simulated cases, which is considered in a safe margin.

Table 6. Optimization results

	S1	S2	S3	S4	S5	S6
T_{ai} [K]	958.5	974	969	953	1053	1052
$\dot{m}_a$ [kg/s]	0.67	0.65	0.66	0.68	0.8	0.8
I [A]	185	180.5	185	185.5	210	210
$\dot{m}_f$ [g/s]	75.6	75.7	76.7	77.6	83.7	83.3
N_{cell}	1876	1770	1762	1800	2388	2381
T_{cell} [K]	1017	1031	1030	1007	1144	1144
P_e [kW]	277	270	264	263	418	416
$\dot{Q}_{net}$ [kW]	254	271	272	261	0	0
FU	0.68	0.64	0.64	0.65	0.8	0.79
η_{el}	0.362	0.34	0.34	0.336	0.495	0.496
η_{sys}	0.729	0.73	0.727	0.70	0.495	0.496
IRR [%]	1.32	0.25	0.46	0.7	0.19	0.64

It is evident from Table 6 that in the scenarios S1-S4 where the thermal power contributes to the revenue the fuel utilization is adjusted to get the best compromise between electrical power output and thermal power output. The optimal FU value varies between 64 and 68% in these scenarios. The maximum FU is obtained for S1, where the cost of electricity is higher and therefore is more convenient to generate more electrical power. The optimal number of cells in S1-S4 is higher for the scenarios with lower C'_{inv}. When the C'_{inv} increases to 2500, the higher investment cost offsets the higher revenue from electricity and therefore we see a lower electrical power production and higher thermal power output. The highest rate of return is obviously observed in

S1 due to the low investment cost and high electricity price.

Since there is no revenue from thermal power in S5 and S6, the optimal FU is the one that results in zero net heat and maximizes power generation. Although the boundaries were set for FU to be lower than 90%, in these scenarios FU never goes above 80% to avoid a negative net heat. In fact, the heat produced by the fuel cell stack is entirely used to pre-heat the air coming into the cathode side. For this reason, the optimal value of T_{ai} is higher than in the scenarios S1-S4, because a higher cell temperature leads to higher power output and it doesn't reduce the revenue since the thermal power is not sold.

The stack current and the number of cells are also higher in S4 and S5 to maximize the electrical power output. The upper limit of stack current was not increased beyond 0.75 A/cm^2 to maintain the accuracy of the trained models. Therefore, the constraints on current and FU caused the achievable power in S5 and S6 to be very close. Unlike the previous scenarios, since the electric power is the only source of revenue, P_e is higher for scenario with higher C'_{inv}, although the return rate is very low at 0.19%. The electrical efficiency is higher for S5 and S6 (~50%) compared to the range of 34% in S1-4, while the overall system efficiency in S5 and S6 is almost half the values in S1-S4. The system efficiency indicated that biogas can be a feasible alternative to natural gas in SOFC systems.

Subsequently, the impact of fuel composition uncertainty on the revenue of the optimized systems was assessed via means of Monte Carlo simulations. The composition was varied in the range presented in Table 1 with the constraint that the sum of all elements fractions should be equal to 1, and 1000 samples were generated. The standard deviation σ of the IRR obtained from the Monte Carlo simulations is shown in Table 7.

Table 7. Uncertainty analysis results

	IRR standard deviation [%]
S1	0.47
S2	0.19
S3	0.18
S4	0.55
S5	0.1
S6	0.22

These results show the need for incorporating fuel composition variations into the optimization procedure, because the uncertainty in IRR induced by the fuel composition is in some cases (S1, S4, and S6) too large to guarantee the economic viability. In particular, higher IRR was observed for higher methane concentration in all scenarios. Scenarios with higher capital investment and lower profit (S2, S3, S5, S6) presented a lower standard deviation since the cost factors had a higher impact on the final IRR, reducing the effect of fuel composition.

CONCLUSIONS

A biogas-fueled SOFC system for micro-grid applications was optimized for six different scenarios. A surrogate model was developed from the data obtained with a 1D dynamic SOFC model, and GA was used to optimize the system design. The optimal number of cells in the stack was observed to be strongly dependent on whether the system was used for cogeneration, more than on the stack cost. The optimal fuel utilization was found in a range of 64-68% for the cogeneration system and around 80% for the purely electrical system. The variability in biogas composition was found to have a significant impact on the economic revenue. The variation in IRR was found statistically significant, with smaller values for higher capital investment. For S1, S4 and S6, the value of 3σ (standard deviation) induced by fuel composition variations is higher than the mean value, which would lead to economic infeasibility. These results prove the need for a robust (as opposed to deterministic) optimization when the biomass characteristics are expected to be highly variable, especially for a future market where the capital cost is expected to decrease.

In future work, a system design that minimizes the impact of fuel composition variability has to be assessed. Uncertainty in the prices of fuel, electricity, and investment cost will also be included.

REFERENCE

[1] Roland Peters, Robert Deja, Maximilian Engelbracht, Matthias Frank, Van Nhu Nguyen, Ludger Blum, Detlef Stolten. Efficiency analysis of a hydrogen-fueled solid oxide fuel cell system with anode off-gas recirculation. Journal of Power Sources 328 (2016) 105-113, Doi:10.1016/j.jpowsour.2016.08.002.

[2] Ozcan H, Dincer I. Performance evaluation of an SOFC based trigeneration system using various gaseous fuels from biomass gasification. Int J Hydrogen Energy 2015. doi:10.1016/j.ijhydene.2014.11.109.

[3] David Hart, Franz Lehner, Stuart Jones, Jonathan Lewis MK. The Fuel Cell Industry Review 2018. E4tech 2018.

[4] Akikur RK, Saidur R, Ping HW, Ullah KR. Performance analysis of a co-generation system using solar energy and SOFC technology. Energy Convers Manag 2014. doi:10.1016/j.enconman.2013.12.036.

[5] Baudoin S, Vechiu I, Camblong H, Vinassa JM, Barelli L. Sizing and control of a Solid Oxide Fuel Cell/Gas Micro Turbine hybrid power system using a unique inverter for

rural microgrid integration. Appl Energy 2016. doi:10.1016/j.apenergy.2016.05.066.
[6] G Mirmoshtaghi, J Skvaril, PE Campana, H Li, E Thorin, E Dahlquist. The influence of different parameters on biomass gasification in circulating fluidized bed gasifiers. Energy Conversion and Management 126 (2016) 110-123.
[7] Mobyen Uddin Ahmed, Peter Andersson, Tim Andersson, Elena Tomas Aparicio, Hampus Baaz, Shaibal Barua, Albert Bergström, Daniel Bengtsson, Daniele Orisio, Jan Skvaril, Jesús Zambrano. A Machine Learning Approach for Biomass Characterization. Energy Procedia 2019.
[8] Recalde Mayra, Woudstra Theo, Aravind P. V. Gasifier, Solid Oxide Fuel Cell Integrated Systems for Energy Production From Wet Biomass. Frontiers in Energy Research 7 (2019) p. 129. DOI 10.3389/fenrg.2019.00129.
[9] Cheng T., Jiang J., Wu X., Li X., Xu M., Deng Z., Li J., Application oriented multi-objective optimization, analysis and comparison of solid oxide fuel cell systems with different configurations, Applied Energy, 2019.
[10] H.A. Reyhani, M. Meratizaman, A. Ebrahimi, O. Pourali, M. Amidpour. Thermodynamic and economic optimization of SOFC-GT and its cogeneration opportunities using generated syngas from heavy fuel oil gasification. Energy 107 (2016) 141-164.
[11] P. Caliandro, L. Tock, A.V. Ensinas, F. Marechal. Thermo-economic optimization of a Solid Oxide Fuel Cell – Gas turbine system fuelled with gasified lignocellulosic biomass. Energy Conversion and Management 85 (2014) 764–773.
[12] Hughes, D., Wepfer, W.J., Davies, K., Ford, J.C., Haynes, C., Tucker, D., A real-time spatial SOFC model for hardware based simulation of hybrid systems, International ASME Conference on Fuel Cell Science, Engineering and Technology, 2011.
[13] Campanari, Thermodynamic model and parametric analysis of a tubular SOFC module, Journal of Power Sources, 2001.
[14] C.A. Salman, M. Naqvi, E. Thorin, J. Yan. Impact of retrofitting existing combined heat and power plant with polygeneration of biomethane: A comparative techno-economic analysis of integrating different gasifiers. Energy Conversion and Management 152 (2017) 250-265. Doi:10.1016/j.enconman.2017.09.022.
[15] C. Pfeifer, S. Koppatz, H. Hofbauer. Steam gasification of various feedstocks at a dual fluidised bed gasifier: Impacts of operation conditions and bed materials. Biomass Conversion and Biorefinery 1(1):39-53. DOI: 10.1007/s13399-011-0007-1.
[16] J. Yao, M. Kraussler, F. Benedikt, H. Hofbauer. Techno-economic assessment of hydrogen production based on dual fluidized bed biomass steam gasification, biogas steam reforming, and alkaline water electrolysis processes. Energy Conversion and Management 145 (2017) 278-292, Doi:10.1016/j.enconman.2017.04.084.
[17] IEA (2020), *Outlook for biogas and biomethane: Prospects for organic growth*, IEA, Paris https://www.iea.org/reports/outlook-for-biogas-and-biomethane-prospects-for-organic-growth
[18] https://www.cell.com/cms/10.1016/j.joule.2019.07.018/attachment/afbdd6b7-5592-4f5e-b704-03608e139670/mmc1.pdf

